Magnetic spin-lattice relaxation in nuclear quadrupole resonance: the eta not=0 case

1991 J. Phys.: Condens. Matter 3 8103

(http://iopscience.iop.org/0953-8984/3/41/009)

J. Phys.: Condens. Matter 3 (1991) 8103–8112. Printed in the UK

Magnetic spin–lattice relaxation in nuclear quadrupole resonance: the $\eta \neq 0$ case

James Chepin and Joseph H Ross, Jr
Department of Physics, Texas A&M University, College Station, TX 77843-4242, USA

Received 7 May 1991

Abstract. We give solutions for spin–lattice relaxation in NQR due to magnetic interactions, generalized for non-axial crystal fields with $\eta \neq 0$. We find analytic expressions for $I = \frac{3}{2}$ and give numerical solutions for $I = \frac{5}{2}$, $\frac{7}{2}$ and $\frac{9}{2}$. We find that the relaxation curves change considerably with η. Specific results are derived for relaxation due to Fermi contact in metals and other electronic hyperfine interactions. We also describe changes induced by the addition of a magnetic field, indicating fields at which standard NMR results break down.

1. Introduction

Spin–lattice relaxation in magnetic resonance offers an excellent probe of dynamical effects in solids, as well as electronic charge carriers accessed via the hyperfine interactions. Relaxation times in nuclear quadrupole resonance (NQR) can be utilised in a similar way as NMR, and these measurements can have great technological importance, for instance in the characterization of polycrystalline metals [1], incommensurate dielectric [2] and anisotropic metals [3], including the high-temperature superconductors [4–6]. For non-axial fields in NQR, however, the energy eigenstates are not identical with magnetic spin states, and the rate equation problem has remained largely unsolved.

The pure quadrupole-Hamiltonian can be written [7]

$$\mathcal{H}_Q = (h\nu_Q/6)[3I_z^2 - I(I+1) + (\eta/2)(I^{+2} + I^{-2})] \tag{1}$$

where spin matrices are represented along the principal axis directions. Here we have $h\nu_Q = 3e^2qQ/[2I(2I-1)]$, and the electric field gradients (EFG's) are contained in eq and η, defined as $eq = V_{zz}$, and $\eta = (V_{xx} - V_{yy})/V_{zz}$. Conventionally, V_{zz} has the largest magnitude, and V_{xx} and V_{yy} are chosen so that $0 \leqslant \eta \leqslant 1$. This is not a necessary assumption in what follows and η can assume any value in our results, as can be convenient for treating 90° axis rotations. However, axial symmetry always implies $\eta = 0$.

We consider magnetic relaxation by weak fluctuating magnetic fields. The nuclear spin coupling to these fields will be written

$$\mathcal{H}_M = \alpha I_z + \beta I_x + \gamma I_y \tag{2}$$

where α, β and γ characterize the field strength and anisotropy. We are therefore assuming that electric quadrupole fluctuations can be neglected, which will be true, for

instance, in metals at low temperatures. Calculations of quadrupole relaxation [8–10] have not been extended to $\eta \neq 0$ NQR.

While the relaxation problem outlined above requires a numerical solution for spins $I > \frac{3}{2}$, we find analytic results for $I = \frac{3}{2}$. We will now describe the general methods, followed in section 3 by solutions for $I = \frac{3}{2}$. Section 4 details results for specific types of relaxation. We give numerical solutions for spins $I > \frac{3}{2}$ in section 5, which can be used to determine the exact behaviour for systems dominated by Fermi contact relaxation. Finally, in section 6 we discuss the behaviour of spin–lattice relaxation with the addition of a magnetic field.

2. Methods

If we define n_i as the difference between the population of the ith level and its equilibrium value, the rate of change of populations is given by a master equation

$$dn_i/dt = \sum_{j \neq i} W_{ij} n_j - n_i \sum_{j \neq i} W_{ij} \tag{3}$$

where

$$W_{ij} = (2\pi/\hbar)\,|\langle i|\mathcal{H}_M|j\rangle|^2. \tag{4}$$

Differences in W_{ij} and W_{ji} due to the lattice temperature are accounted for as usual [7] by including equilibrium populations in n_i. Note that the Andrew-Tunstall [11] result for NMR, $W_{m,m-1} = W(I+m)(I-m+1)$, *cannot* be used here (this form holds for cylindrical symmetry only, a point that has not always been made clear in the literature). Expression of this problem in terms of fictitious-spin-$\frac{1}{2}$ operators [12, 13] is also difficult since energy states in the present case are not I_z eigenstates. In general, the I_x and I_y matrix elements change with η, and we must keep the I_z terms in NQR.

For classical fluctuating fields, the rates (4) should be modified to include only the spectral density weighted at the transition frequency [7]. In what follows we assume that the spectral density is independent of the transition frequency (correlation time larger than $1/\nu_L$). This is most appropriate for the high-temperature regime, above the T_1 minimum temperature. The numerical method described below can be generalized, though, to include the lower-temperature weak-collision regime. (For electron hyperfine interactions in metals, spectral densities will typically be constant at all temperatures; a modified rate expression appropriate for electron hyperfine coupling is discussed below.)

States i and j are eigenstates of the quadrupole Hamiltonian, (1); for $\eta = 0$ these are eigenstates of I_z, and the resulting spin–lattice recovery curves have been determined for all half-integer spins by MacLaughlin *et al* [8]. For the more general case $\eta \neq 0$, we have utilized the symbolic programming system, *Mathematica*, to find analytic solutions for $I = \frac{3}{2}$ and numerical solutions for other spins.

A convenient representation for the master equations (3) is in matrix form

$$d\boldsymbol{n}/dt = \mathbf{A} \cdot \boldsymbol{n} \tag{5}$$

where $A_{ij} = W_{ij} - \Sigma W_{ij}\delta_{ij}$ is the $(2I+1) \times (2I+1)$ relaxation matrix. The solution to (5) is a multi-exponential spin–lattice relaxation curve, with exponents given by the eigenvalues of $\mathbf{A}$, and coefficients determined from the initial experimental preparation (e.g. saturation of a specified transition). The multiexponential relaxation is homogeneous and the result of non-uniformly spaced levels that cannot achieve a common spin

temperature. A standard method [8, 14, 15] has been to define population differences between adjacent levels in place of $\boldsymbol{n}$ and to rewrite equation (5) accordingly. For $\eta \neq 0$ NQR, $\mathbf{A}$ is not a sparse matrix, and this procedure becomes non-trivial. We therefore keep the level populations themselves as the quantities of interest. In this case, the eigensystem of $\mathbf{A}$ includes one vector with all equal elements and zero eigenvalue, which is the unchanging total population (always zero in the high-temperature approximation for the traceless Hamiltonian (1)).

3. Exact solutions for $I = \frac{3}{2}$

We find that for $I = \frac{3}{2}$ the normalized eigenstates for the Hamiltonian (1) can be written

$$\Psi_1 = \{-\mathrm{i}a, -b, \mathrm{i}b, a\} \tag{6a}$$

$$\Psi_2 = \{\mathrm{i}a, -b, -\mathrm{i}b, a\} \tag{6b}$$

$$\Psi_3 = \{\mathrm{i}b, a, \mathrm{i}a, b\} \tag{6c}$$

$$\Psi_4 = \{-\mathrm{i}b, a, -\mathrm{i}a, b\} \tag{6b}$$

where $\mathrm{i} = \sqrt{-1}$, and a and b are given by:

$$a = [(9 + 3\eta^2)^{1/2} - 3]^{1/2}/(2\sqrt{3}) \tag{7a}$$

$$b = [(9 + 3\eta^2)^{1/2} + 3]^{1/2}/(2\sqrt{3}). \tag{7b}$$

The states (6) are in the I_z basis, in which the $m = \frac{3}{2}, \frac{1}{2}, -\frac{1}{2}$ and $\frac{3}{2}$ states are $\{1, 0, 0, 0\}$, $\{0, 1, 0, 0\}$, $\{0, 0, 1, 0\}$ and $\{0, 0, 0, 1\}$, respectively. States Ψ_1 and Ψ_2 have energy eigenvalue $-h\nu_Q(9 + 3\eta^2)^{1/2}/6$, and states Ψ_3 and Ψ_4 have eigenvalue $+h\nu_Q(9 + 3\eta^2)^{1/2}/6$. Other linear combinations of the degenerate states can be chosen, however we find that the states (6) diagonalize the perturbation (2), and therefore are most appropriate.

The relaxation matrix $\mathbf{A}$ can be determined from the spin-state eigensystem (6) and the perturbation (2). We find that only one of the four eigenmodes of $\mathbf{A}$ produces population changes observable in NQR. In the energy state basis $\{\Psi_1, \Psi_2, \Psi_3, \Psi_4\}$ (as opposed to the I_z basis used above), the observable NQR mode is in all cases $\{1, 1, -1, -1\}$, and thus removes population from the degenerate states (Ψ_3, Ψ_4) and adds population to the degenerate states (Ψ_1, Ψ_2). The spin–lattice relaxation is single-exponential, described by the curve $\exp(-\rho t)$, where ρ is the eigenvalue corresponding to the mode described above. We find

$$\rho = \alpha^2\, 2\eta^2/(3+\eta^2) + \beta^2(3+\eta)^2/[2(3+\eta^2)] + \gamma^2(3-\eta)^2/[2(3+\eta^2)]. \tag{8}$$

Note that there are no cross terms in (8), so that correlated fluctuations do not modify the results. (We have verified the latter only for α, β and γ having the same phase, as would be expected for nonmagnetic material with time-reversal symmetry.) Correlation of the fields α, β and γ could correspond to fluctuations whose principal axes differ from the EFG principal axes. Fluctuations on any axis can therefore be treated for $I = \frac{3}{2}$ by taking components (α, β and γ) resolved into the EFG principal axis system and inserting these components into (8).

4. Specific relaxation effects

We now demonstrate the application of these results to specific cases, including hyperfine interactions in metals.

4.1. Classical isotropic fluctuations

The relaxation rate (8) simplifies greatly when isotropic magnetic fluctuations are the dominant relaxation process, so that $\alpha = \beta = \gamma$. The Hamiltonian (2) can be regarded in this case as $(\boldsymbol{I} \cdot \boldsymbol{H}_{\rm loc})$, where $\boldsymbol{H}_{\rm loc}$ is a local field due, for instance, to the untruncated dipolar interaction. The rate (8) then becomes $\rho = 3\alpha^2$, independent of η. This rate is three times the usual definition of $(T_1)^{-1}$, or three times the smallest exponent measured in an NMR experiment under the same conditions. We find a similar result for the Fermi contact interaction described below. However, in section 5 we show that relaxation curves depend strongly on η even for isotropic fluctuations for spins $I > \frac{3}{2}$.

4.2. Fermi contact interaction in metals

The Fermi contact Hamiltonian in metals is given by [7]

$$\mathcal{H}_{\rm FC} = (2/3\pi)\delta(\boldsymbol{r})\gamma_{\rm e}\gamma_{\rm n}\hbar^2[I_z S_z + \tfrac{1}{2}(I^+S^- + I^-S^+)] \tag{9}$$

where S operators are for electron spin, and I operators are for nuclear spin. To determine the effective matrix elements for nuclear spin relaxation, we must sum over all electron states:

$$W_{ij} = \frac{4\pi^2}{h} \sum_{k,\sigma,k',\sigma'} |\langle ik\sigma|\, \mathcal{H}_{\rm FC}\, |jk'\sigma'\rangle|^2\, \delta(\varepsilon_{k\sigma} - \varepsilon_{k'\sigma'}) f(\varepsilon_{k\sigma})[1 - f(\varepsilon_{k'\sigma'})]. \tag{10}$$

In (10), k and σ refer to electron orbital and spin states, respectively, and $f(\varepsilon_{k\sigma})$ is a Fermi function.

For simple non-magnetic metals we can write the states $|ik\sigma\rangle$ as product states, $|i\rangle\,|k\rangle\,|\sigma\rangle$. The sum over k states can be performed immediately, giving

$$\begin{aligned} W_{ij} = W_o[4|\langle i|I_z|j\rangle|^2(|\langle +|S_z|+\rangle|^2 + |\langle -|S_z|-\rangle|^2) \\ + |\langle i|I^+|j\rangle|^2|\langle -|S^-|+\rangle^2 + |\langle i|I^-|j\rangle|^2|\langle +|S^+|-\rangle|^2] \end{aligned} \tag{11}$$

where

$$W_o = \tfrac{4}{3}h^3kT[\gamma_{\rm e}\gamma_{\rm n}\rho(\varepsilon_{\rm F})]^2\langle u(0)\rangle^2$$

is equivalent to $(2T_1)^{-1}$ in the standard definition [7], in which $(T_1)^{-1}$ is the smallest exponent for NMR relaxation. Note that this differs from the cylindrical-symmetry result in that the I_z matrix elements have been retained. The electron spin matrix elements are shown explicitly in (11) in terms of the electron spin states $|+\rangle$ and $|-\rangle$. Evaluating these terms yields

$$\begin{aligned} W_{ij} &= W_o[2|\langle i|I_z|j\rangle|^2 + |\langle i|I^+|j\rangle|^2 + |\langle i|I^-|j\rangle|^2] \\ &= 2W_o[|\langle i|I_z|j\rangle|^2 + |\langle i|I_x|j\rangle|^2 + |\langle i|I_y|j\rangle|^2]. \end{aligned} \tag{12}$$

While the result (12) is general, a specific form for $I = \frac{3}{2}$ can easily be obtained.

Comparing the result (12) to the definition (2) above we may define effective field strengths for the fermi contact interaction, $\alpha = \beta = \gamma = (2W_o)^{1/2}$, and use these in (8) to determine the relaxation rate. This equivalence is possible since the relaxation rate (8) contains no cross terms, which are excluded from the transition probabilities (12) calculated above. The result is a relaxation rate $\rho = 6W_o$. This is independent of η, and is identical to the result found previously [8] for $\eta = 0$. Note that this is specific to $I = \frac{3}{2}$, as for isotropic classical fluctuations; elsewhere we demonstrate that a T_1 independent of η is not the rule.

4.3. Other hyperfine interactions in metals

Because the core polarization interaction [16] depends upon Fermi contact between *s*-core states and the nuclei, this interaction will produce transition rates equivalent to (12), with a prefactor containing the relevant hyperfine coupling constant. It is clear, however, that orbital and dipolar hyperfine couplings in anisotropic metals will cause transition rates that depend in a detailed way on the form of the nuclear eigenstates.

For a dipolar interaction, it is easily shown that for a single orbital at ε_F of the form Y_l^0 (quantised about z), the standard expression [17] for the dipolar interaction yields transition rates of the form

$$W_{ij} \propto \{2|\langle i|I_z|j\rangle|^2 + |\langle i|I_x|j\rangle|^2 + |\langle i|I_y|J\rangle|^2\}. \tag{13}$$

The resulting relaxation rate for $I = \frac{3}{2}$ can be shown from (8) to depend on η for this specific case as $(5\eta^2 + 9)/(3 + \eta^2)$. We see therefore that the magnetic relaxation rate measured in NQR depends in a detailed way on the symmetry.

Orbital relaxation results from hyperfine couplings of the form $\boldsymbol{I} \cdot \boldsymbol{L} = [I_z L_z + \frac{1}{2}(I^+L^- + L^-L^+)]$. For $I = \frac{3}{2}$, the relaxation rate can be determined directly from (8) if the mixture of orbitals at ε_F is known. Unless all m states are equally populated (which implies spherical symmetry), the rate will not always be $6W_o = 3/T_1$. For low-symmetry metals having non-axial EFGs, unfilled states at the Fermi level will likely involve fewer orbitals than the cubic and hexagonal cases treated by Obata [17]. For instance, if we consider one-dimensional conductors with pure d_{z^2} conduction bands [18], all relevant L^+, L^-, and L_z matrix elements vanish, leaving no orbital contribution to the spin–lattice relaxation. However, a mixture of $m = \pm 1$ orbitals will give a non-zero contribution due to L^+ and L^- terms. For instance, the addition of a small $d_{xy} = (Y_2^1 + Y_2^{-1})$ orbital gives a non-zero transition rate proportional to $|\langle i|(I^+ + I^-)/2|j\rangle|^2 = |\langle i|I_x|j\rangle|^2$, so that the β term in (8) determines the relaxation rate. Note that the crystal field will usually quench m states, so that matrix elements of L^+ and L^- cannot be treated independently, as were the S^+ and S^- elements above.

5. Numerical results for $I > \frac{3}{2}$

It is not possible to find the analytic solution analogous to (8) for spins $I > \frac{3}{2}$ (even utilizing the double-degeneracy for NQR to reduce the spin matrix by one half). Instead, we have solved the eigenvalue problem numerically for different values of the asymmetry parameter, η, using for these calculations the numerical linear algebra facilities in *Mathematica*. We developed a programming package so that this can be

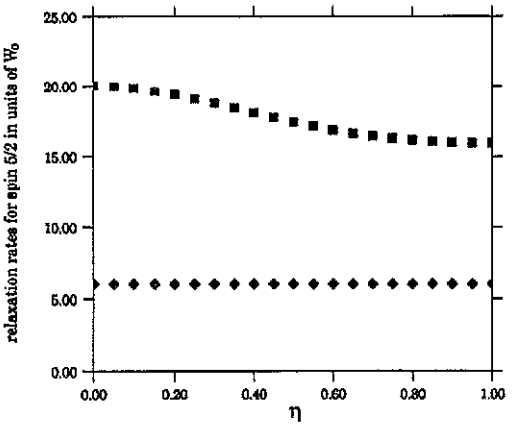

Figure 1. Relaxation rates vs. η for spin $\frac{5}{2}$, in units of W_0 (defined in the text), for Fermi contact interaction.

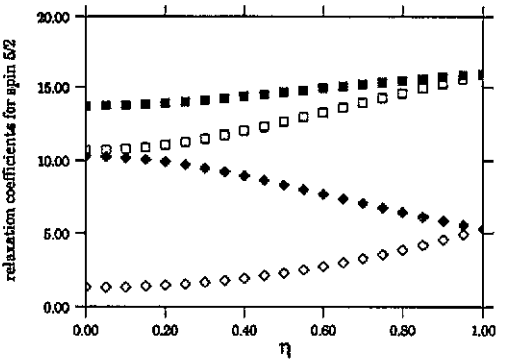

Figure 2. Exponential coefficients for spin $\frac{5}{2}$ as a function of η. The '$\frac{5}{2}$–$\frac{3}{2}$' and the '$\frac{3}{2}$–$\frac{1}{2}$' transitions are represented by filled and open symbols, respectively. The symbols correspond to those with the same shape used for the rates in figure 1. Coefficient scaling is described in the text.

done for any half-integer spin, keeping all degenerate states. This approach also allows us to add a static Zeeman field to the problem, as described in section 6.

For spins $\frac{5}{2}$, $\frac{7}{2}$ and $\frac{9}{2}$ magnetic relaxation in NQR is multi-exponential. The problem of the relative strength of each mode must therefore be addressed by expanding the initial population differences, $\boldsymbol{n}_0$, in terms of the eigenmodes of $\mathbf{A}$. Note that three representations of the state of the system are available: the I_z basis, the energy-state basis and the basis of eigenmodes of $\mathbf{A}$. We calculate the energy eigenvalues in the I_z representation and then calculate matrix elements of $\mathcal{H}_M$ to give $\mathbf{A}$ in the energy-state basis.

Equilibrium energy-state populations were assumed proportional to the energy of each state, in a high temperature approximation. For an inversion of the transition between two given *pairs* of degenerate states, we interchanged the populations of the four states involved and subtracted the equilibrium populations to find the initial population differences, $\boldsymbol{n}_0$. Thus for a transition between states (Ψ_1, Ψ_2) and states (Ψ_3, Ψ_4) for spin $I = \frac{5}{2}$, the initial vector is $\boldsymbol{n}_0 = \{\delta E, \delta E, -\delta E, -\delta E, 0, 0\}$ in the energy-state basis, where $\delta E = (E_3 - E_1)$. The coefficients described below thus are scaled by the state energies (which depend on η).

Defining $\mathbf{C}$ as the matrix whose columns are normalized normal modes of $\mathbf{A}$ (similar to Narath's [15] notation), $\boldsymbol{n}_0$ weighted in the normal mode basis is equal to $\mathbf{C}^{-1} \cdot \boldsymbol{n}_0$, where $\mathbf{C}^{-1}$ is the inverse of $\mathbf{C}$ (equal to its transpose). Each mode decays exponentially, so that at time t, mode i has strength $(\mathbf{C}^{-1} \cdot \boldsymbol{n}_0)_i \exp(-\rho_i t)$, where ρ_i is the corresponding eigenvalue of $\mathbf{A}$. The time-dependent energy-state populations, $\boldsymbol{n}(t)$, are found by multiplying by the matrix of eigenmodes which transforms the populations to the energy-state basis:

$$\boldsymbol{n}_i(t) = \sum_j \mathbf{C}_{ij}(\mathbf{C}^{-1} \cdot \boldsymbol{n}_0)_j \exp(-\rho_j t).$$

Finally, the NQR signal is given by subtracting the population differences of the states under observation.

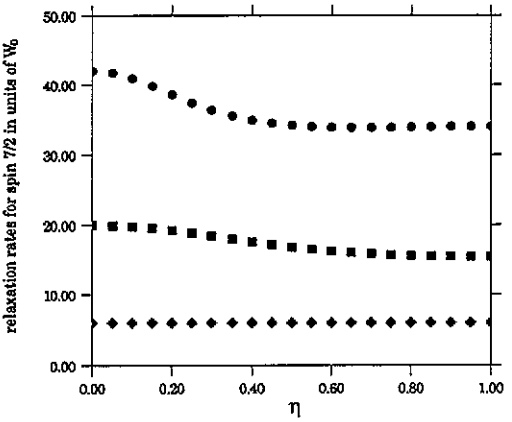

Figure 3. Relaxation rates vs. η for spin $\frac{7}{2}$, in units of W_0 (defined in the text), for Fermi contact interaction.

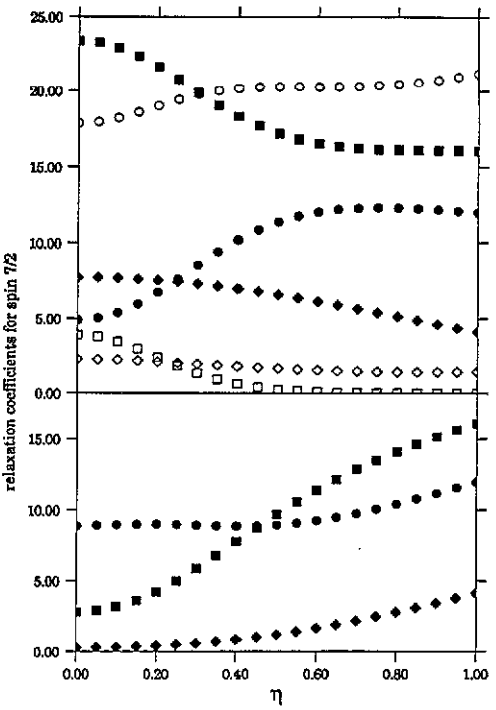

Figure 4. Exponential coefficients for spin $\frac{7}{2}$ as a function of η. The upper portion of the figure shows the '$\frac{7}{2}$–$\frac{5}{2}$' and the '$\frac{5}{2}$–$\frac{3}{2}$' transition coefficients using filled and open symbols, respectively. The lower portion contains the '$\frac{3}{2}$–$\frac{1}{2}$' transition coefficients. The symbols correspond to those with the same shape used for the rates in figure 3. Coefficient scaling is described in the text.

For $\eta = 0$, eigenvalues ρ_i are given by [8] ($6W_o$, $20W_o$) for $I = \frac{5}{2}$, ($6W_o$, $20W_o$, $42W_o$) for $I = \frac{7}{2}$, and ($6W_o$, $20W_o$, $42W_o$, $72W_o$) for $I = \frac{9}{2}$, where $2W_o$ is equal to $1/T_1$ as usually defined. These NQR eigenvalues correspond to eigenmodes of **A** that have even symmetry under coordinate reversal, whereas the modes observable in NMR have odd symmetry. For $\eta \neq 0$, with no Zeeman field, this symmetry is unchanged, so that the number of modes for NQR relaxation is restricted to 2, 3 and 4 for $I = \frac{5}{2}$, $\frac{7}{2}$ and $\frac{9}{2}$ respectively.

We have calculated relaxation exponents and coefficients specifically for the Fermi contact relaxation, for which the matrix elements have been determined in section 4.2. For metals dominated by the contact interaction, exact relaxation curves can be obtained from figures 1–6, where relaxation exponents are reported in terms of W_o, and the coefficient for each exponential is in relative units, scaled by the transition frequency as described above. Transitions are defined according to the I_z states that hold for $\eta = 0$ (e.g. '$\frac{5}{2}$—$\frac{7}{2}$' transition); these states change smoothly with η. We show only those transitions that correspond to observable transitions for $\eta = 0$. Although the exponents change with η in nearly the same way for each spin, they are not

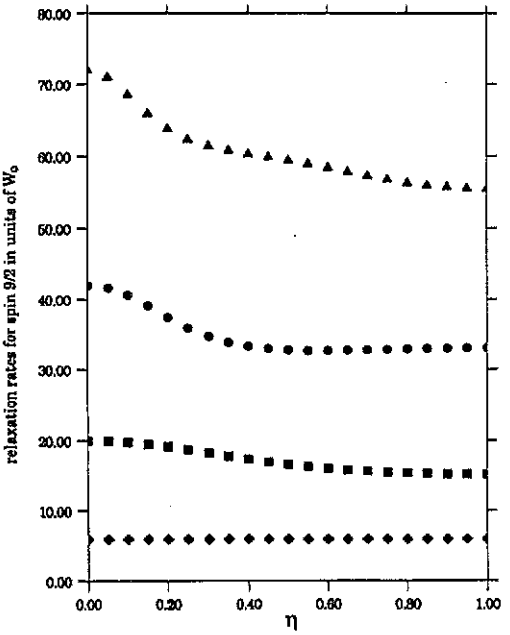

Figure 5. Relaxation rates vs. η for spin $\frac{9}{2}$, in units of W_0 (defined in the text), for Fermi contact interaction.

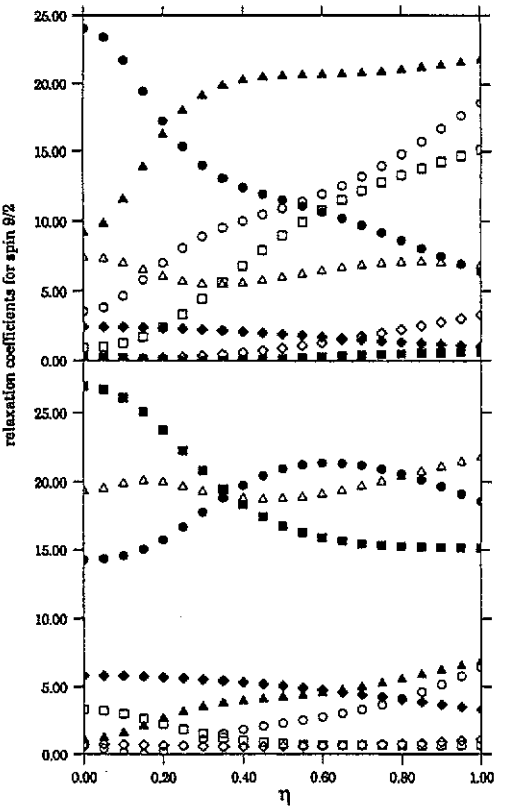

Figure 6. Exponential coefficients for spin $\frac{9}{2}$ as a function of η. The upper portion of the figure shows the '$\frac{7}{2}$–$\frac{9}{2}$' and the '$\frac{5}{2}$–$\frac{7}{2}$' transition coefficients using filled and open symbols, respectively. The '$\frac{3}{2}$–$\frac{5}{2}$' and the '$\frac{1}{2}$–$\frac{3}{2}$' transition coefficients are in the lower portion, shown using filled and open symbols, respectively. The symbols correspond to those with the same shape used in figure 5 for the relaxation rates. Coefficient scaling is described in the text.

identical. However, our results show that for the contact interaction, the smallest exponent equals $6W_o$ for all cases, which includes the $I = \frac{9}{2}$ result already described. Other exponents are not constant. (For anisotropic fluctuations, this smallest exponent becomes a function of η, as well.)

Therefore, if the relaxation is of the contact type, we demonstrate that the long-time tail of the relaxation curve can be fitted to the exponent $6W_o$, independent of the details of the EFG tensor. This result may be useful to characterize disordered metals, in which η can be distributed inhomogeneously. However, many of the $6W_o$ coefficients are small. Furthermore, the full relaxation curve, with coefficients and rates given in figures 1–6, contains information about the relaxation mechanism. Our results give the exact zero-field relaxation behaviour for simple metals with anisotropic EFG's.

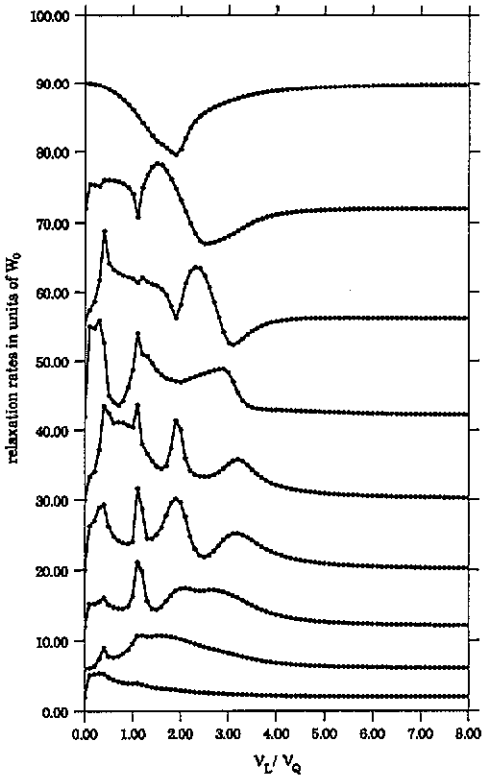

Figure 7. Dependence of the relaxation rates upon a magnetic field along the quadrupolar z symmetry axis for spin $\frac{9}{2}$ and $\eta = 1$. Relaxation is via Fermi contact interaction. Rates have units of W_0 (defined in the text).

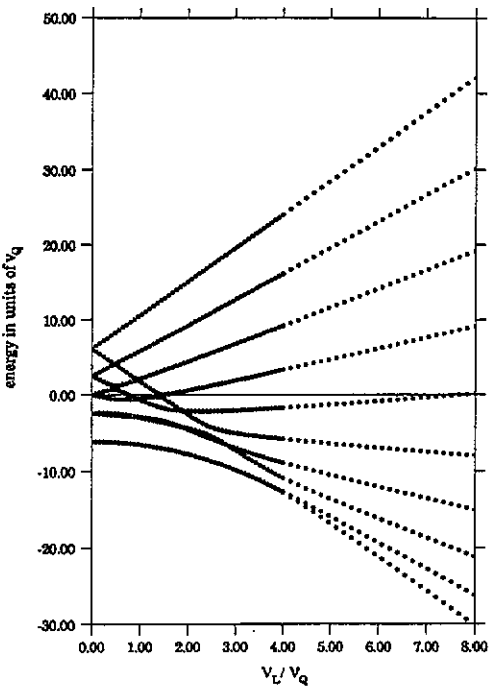

Figure 8. Energy states of a spin $\frac{9}{2}$ nucleus in a completely antisymmetric ($\eta = 1$) quadrupolar field as a function of an applied magnetic field along the z symmetry axis.

6. Addition of a magnetic field

With the addition of a static magnetic field, the energy eigenstates become equivalent to pure I_z states in the high field limit. We show that the approach to the high field limit is not simple or smooth in the region $\nu_Q = \nu_L$, where $\nu_L = \gamma H_0/2\pi$ is the Larmor frequency.

The magnetic field adds a Zeeman term $\mathcal{H}_Z = h\nu_L I_z$ to the Hamiltonian (1). The numerical procedure outlined above can be followed if we replace the energy states by those of the new Hamiltonian. The Zeeman term destroys the inversion symmetry of the Hamiltonian, and as a result all eigenmodes contribute to the observed relaxation curve (e.g. nine exponentials for $I = \frac{9}{2}$ of which five are important in high fields).

In figure 7 are shown exponents calculated for $I = \frac{9}{2}$, for the addition of a Zeeman Hamiltonian $\mathcal{H}_z = h\nu_L I_z$, corresponding to a magnetic field along the z-EFG principal axis. These curves were calculated specifically for a contact interaction, as in figures 1–6, and for a fixed orientation of the EFG's, with $\eta = 1$. The energies for this situation are shown in figure 8. Prominent peaks and changes in the rates in figure

7 can be identified with energy-level anti-crossings. Clearly, in these regions the eigenstates become strongly mixed, thereby modifying the relaxation matrix **A**. Note that more than one rate is affected strongly by each level crossing since the eigenmodes of **A** are mixtures of energy states. The spin–lattice relaxation for *all* transitions thus exhibits this structure, including transitions between higher-energy states whose energies change smoothly over the entire range. Changes with field becomes smaller as η approaches zero, until finally level anti-crossings will vanish for $\eta = 0$. For the non-axial case, however, the rates approach the high-field limit only above the highest-field anti-crossing, or above a maximum Larmor frequency of approximately ν_Q, $2\nu_Q$, $3\nu_Q$ and $4\nu_Q$, for $I = \frac{3}{2}, \frac{5}{2}, \frac{7}{2}$ and $\frac{9}{2}$ respectively. Thus we demonstrate explicitly the magnetic fields for which standard NMR results can be utilized in $\eta \neq 0$ quadrupole systems.

References

[1] Abart J, Palangié E, Socher W and Voitländer J 1983 *J. Chem. Phys.* **78** 5468
[2] Chen S and Ailion D C 1989 *Solid State Commun.* **69** 1041
[3] Suits B H and Slichter C P 1984 *Phys. Rev.* B **29** 41
[4] Pennington C H, Durand D J, Slichter C P, Rice J P, Bukowski E D and Ginsberg D M 1989 *Phys. Rev.* B **39** 2902
[5] Walstedt R E, Warren W W Jr, Bell R F and Espinosa G P 1989 *Phys. Rev.* B **40** 2572
[6] Monien H, Pines D and Slichter C P 1990 *Phys. Rev.* B **41** 11 120
[7] Slichter C P 1990 *Principles of Magnetic Resonance* 3rd edn (Berlin: Springer)
[8] MacLaughlin D E, Williamson J D and Butterworth J 1971 *Phys. Rev.* B **4** 60
[9] Gordon M I and Hoch M J R 1978 *J. Phys. C: Solid State Phys.* **11** 783
[10] Rega T 1991 *J. Phys.: Condens. Matter* **3** 1871
[11] Andrew E R and Tunstall D P 1961 *Proc. Phys. Soc.* **78** 1
[12] Vega S 1978 *J. Chem. Phys.* **68** 5518
[13] Petit D and Korb J-P 1988 *Phys. Rev.* B **37** 5761
[14] Simmons W W, O'Sullivan W J and Robinson W A 1962 *Phys. Rev.* **127** 1168
[15] Narath A 1967 *Phys. Rev.* **262** 320
[16] Yafet Y and Jaccarino V 1964 *Phys. Rev.* **133** 1630
[17] Obata Y 1963 *J. Phys. Soc. Japan* **18** 1020
[18] Canadell E, Rachidi I E-I, Pouget J P, Gressier P, Meerschaut A, Rouxel J, Jung D, Evain M and Whangbo M-H 1990 *Inorg. Chem.* **29** 1401